Directional selection can drive the evolution of modularity in complex traits

Diogo Melo[1] and Gabriel Marroig

Departamento de Genética e Biologia Evolutiva, Instituto de Biociências, Universidade de São Paulo, Sao Paulo, SP 05508-090, Brazil

Modularity is a central concept in modern biology, providing a powerful framework for the study of living organisms on many organizational levels. Two central and related questions can be posed in regard to modularity: How does modularity appear in the first place, and what forces are responsible for keeping and/or changing modular patterns? We approached these questions using a quantitative genetics simulation framework, building on previous results obtained with bivariate systems and extending them to multivariate systems. We developed an individual-based model capable of simulating many traits controlled by many loci with variable pleiotropic relations between them, expressed in populations subject to mutation, recombination, drift, and selection. We used this model to study the problem of the emergence of modularity, and hereby show that drift and stabilizing selection are inefficient at creating modular variational structures. We also demonstrate that directional selection can have marked effects on the modular structure between traits, actively promoting a restructuring of genetic variation in the selected population and potentially facilitating the response to selection. Furthermore, we give examples of complex covariation created by simple regimes of combined directional and stabilizing selection and show that stabilizing selection is important in the maintenance of established covariation patterns. Our results are in full agreement with previous results for two-trait systems and further extend them to include scenarios of greater complexity. Finally, we discuss the evolutionary consequences of modular patterns being molded by directional selection.

variational modularity | G-matrix | quantitative genetics | pleiotropy | phenotypic correlations

Modularity, the organizational pattern found in many organisms, can be defined as the tendency for some parts to be more associated with each other than with other parts of the same organism. This type of modular organization can manifest at many levels, for example, between the bases of an RNA molecule (1), in the interaction between proteins (2), or in the covariance structure of continuous morphological traits (3). In each case, the type of association is different, but the modular pattern remains (4). Traits measured on a continuous scale that covary with each other can frequently be divided into variational modules. A variational module is characterized by higher correlations between traits in the same module and lower correlations between traits of different modules.

Modularity is an important concept in understanding the evolution of many biological systems. At the individual level, tension in producing a full, coherent organism, and having each of its parts performing a separate task subject to different selective pressures and requirements, shapes the association between traits (5). At the same time, the existing pattern of association also influences the response to a given selective pressure: Traits that are associated tend to change together (6, 7). The evolutionary consequences of these correlations are twofold. On the one hand, traits that perform a common function will tend to change in an orchestrated fashion, although interfering less with traits in other modules at the same time. On the other hand, if natural selection promotes changes in only one trait of a module, the other traits within this module will suffer an indirect selection pressure and change as well, even if this response leads to lower fitness (8). This indirect response in other traits is due to their genetic correlation with the selected trait. Understanding how traits become associated, or correlated, is therefore a central question in evolutionary biology.

The question of how modular patterns evolve in each level of complexity is still open to intense scrutiny (9–11). In morphological systems, one condition for the evolution of variational pattern is the existence of genetic variation in the association between traits in a population. Pavlicev et al. (12) have presented empirical evidence of this variation by showing the existence of relationship quantitative trait loci (rQTLs). These rQTLs are genomic regions that show variation in epistatic effects, altering pleiotropic relations and the correlation between phenotypic traits. Using this concept and the multivariate breeder's equation, Pavlicev et al. (13) proposed a simple deterministic model for the evolution of association or dissociation between two traits in response to directional and stabilizing selection.

The variational pattern of genetic associations between continuous morphological traits is expressed in the additive genetic covariance matrix, called the G-matrix (8, 14). Covariance expressed in the G-matrix is the result of the sum and interaction of genetic effects on many traits, such as pleiotropic and epistatic effects, and shared development, leading to heritable variation and covariation. This variation interacts with evolutionary processes, such as drift and selection. The multivariate breeder's equation relates a population's G-matrix with its response to a given directional selection pressure (14). Under certain conditions,

---

Significance

Modularity, the tendency for the parts of many biological systems to be organized into semiindependent groups, is crucial to the understanding of diversification and the interaction between a population and its environment. In particular, a population's response to selection is dependent on its modularity pattern, which, in turn, is molded by selection. How these modular patterns evolve is therefore a central question in biology. We show, using novel individual-level simulations, that directional selection is very efficient at restructuring variation and creating modular patterns in continuous traits and that stabilizing selection can maintain established patterns.

mainly the stability of the G-matrix over many generations, we may use this equation to infer the net selection pressures responsible for a given differentiation between populations (15). So, the question of stability of the G-matrix under different conditions is relevant for understanding natural diversification of populations and species. A sequence of articles by Jones et al. (15–18) investigates this problem using stochastic individual-based computer simulations under various conditions, including directional and stabilizing selection, drift, and mutation. However, these articles focus on two traits, mostly using a stable mutation correlation matrix (a proxy of the pleiotropic/epistatic relations), except in two articles (17, 18). Jones et al. (17, 18) show that stabilizing selection is capable of creating and maintaining an association between two quantitative traits by influencing the mutation correlation matrix of the populations. If the correlation matrix for mutational effects is kept constant, its alignment with stabilizing selection will also maintain the correlation between two traits (16). In addition, correlated directional selection can help maintain stable associations when aligned with variation in the population and the mutation correlation matrix (15).

These results give valuable insight into the problem of the evolution of modularity. However, investigating the two-trait case with a stable developmental scheme can be limiting when we are interested in the evolution of modularity. With two traits, complex modular relationships cannot arise, and without a changing genotype-to-phenotype map, no substantial change can occur in the heritable variation pattern. Although some articles investigate more than two traits (19) or an evolving mutation matrix (17, 18), to the best of our knowledge, no effort has been made to combine these two complications. We attempt to fill this gap, presenting a model capable of simulating many traits controlled by many loci with variable relations between them, expressed in populations subject to mutation, recombination, drift, and selection (Fig. 1). We use this model to study the problem of emergence of modularity in a system with 10 continuous phenotypic traits divided into two potential variational modules composed of five traits, as well as the interaction between

Fig. 1. Pictorial representation of the simulation scheme. Dynamics for a single individual in the population. In this example, two loci (**y**, $m = 2$) control the additive values for two traits (**x**, $p = 2$), with the pleiotropic **B** matrix connecting these two levels. To obtain the phenotype (**z**), additive values are added to Gaussian noise (**e**). Phenotypic values are then used to attribute a fitness to each individual, according to a Gaussian selection surface defined by the peak θ and covariance matrix ω. Mating pairs are sampled with a probability proportional to their fitness, and gametes formed by sampling one allele from each locus, along with their pleiotropic effects expressed in the **B** matrix. Mutation can alter the values of each element of **y** with probability μ by an amount drawn from a Gaussian distribution with a mean of 0 and variance σ; and mutation can also add or remove arrows connecting **y** to the additive values in **x** with probability μ_B. Mutation acts before the formation of gametes but after selection.

covariation patterns and selection. To facilitate comparison with existing observational data, we focus on phenotypic covariance matrices, not genetic ones. Phenotypic matrices are much easier to measure, and G-matrix estimates are frequently impossible to obtain. Here, they are proportional, and because phenotypic matrices include environmental noise, phenotypic module detection is a stricter test for modularity in our simulations.

Results

Initial Population. Our first step was to establish a baseline population after a long burn-in period to serve as a starting point for all populations. We generated a random population, described in *SI Appendix*, and subjected it to 10,000 generations of random genetic drift without selection. Then, the same population was subjected to 10,000 generations of uncorrelated stabilizing selection with a diagonal selection surface covariance matrix and a stable peak. We also performed a subset of the simulations with random initial populations, repeating the burn-in periods of drift and stabilizing selection for each population to assess whether the results were sensitive to the starting populations, and no such effect was found (*SI Appendix*, Figs. S5 and S6). Because this burn-in period adds considerable computational time (a factor of 3), we opted to use the same starting population for all simulations.

Random Genetic Drift. After the burn-in period, we removed the selection on the populations, subjecting them to random drift. This procedure is essentially a null test to verify that the absence of selection would not lead to the kind of modular organization found in the simulations discussed below. We ran 50 replicates of 10,000 generations of drift, and no modular pattern consistent with our modularity hypothesis was established by genetic drift alone, as seen in the ratio of within- and between-module average phenotypic correlations [average ratio (AVG Ratio); *Materials and Methods* and *SI Appendix*, Fig. S2]. At the end of 10,000 generations, the highest observed value for the AVG Ratio was around 1.1, with most values falling closer to 1 or less. This value indicates no differentiation in the average values of correlations within and between modules, and no evidence of variational modularity.

Stabilizing Selection. Starting with the same initial population, we ran 50 runs of correlated stabilizing selection, using a nondiagonal selection surface covariance matrix, with a correlation of 0.8 within modules (traits 1–5 and 6–10) and zero between modules and a variance of 10 for all modules, which corresponds to strong stabilizing selection (*SI Appendix*, Figs. S8 and S9). A slight modular pattern was established over the experimental runs, and at the end of 10,000 generations, most populations maintained AVG Ratios over 1.0 and many were in the range of 1.1–1.2 (*SI Appendix*, Fig. S2).

Divergent Directional Selection. To investigate the effect of directional selection, we subjected the populations to divergent directional selection on all traits. We imposed changes in the selection surface peak at a fixed rate per generation, causing the mean of the population to be dislocated from the peak and, consequently, to experience directional selection. These changes ranged from very weak to moderate but were sustained for many generations, causing significant morphological differences. Traits 1–5, in the first module, were subjected to selection in one direction, toward negative trait values. Accordingly, traits 6–10, in the second module, were subjected to directional selection in the other direction, toward positive trait values. All populations responded to directional selection with changes in their means.

When under divergent directional selection of sufficient strength, the between-module phenotypic correlation dropped to nearly 0 and the within-module correlation rose (Fig. 2 and *SI Appendix*, Fig. S3). Stronger selection led to more differentiation between modules. In addition to the AVG Ratio, changes in the eigenvalue structure
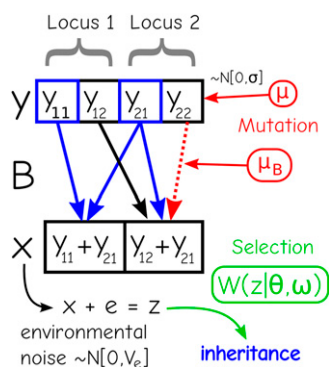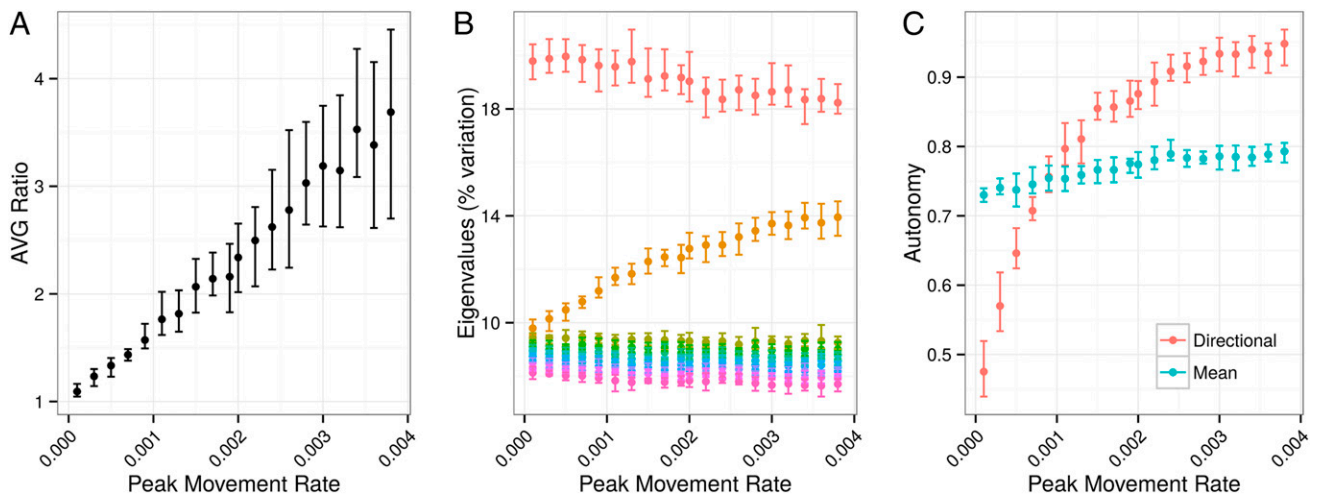
Fig. 2. Populations under divergent directional selection. (*A*) Ratio of average within- and between-module phenotypic correlations (AVG Ratio) under increasing correlated peak movement rate. The AVG Ratio increases with peak movement rate, indicating more differentiation of within- and between-module correlations. Variance of the AVG Ratio within populations for a given peak movement rate increases with the rate because between-module correlations get progressively smaller, leading to a divergence in AVG Ratio. (*B*) Percentage of variation explained by each eigenvalue. Each color represents an eigenvalue, ordered from top to bottom. As the divergent peak movement rate increases, variation associated with dissociation between modules increases (the second principal component, a contrast between modules; *SI Appendix*). (*C*) Mean and directional autonomy for various peak movement rates. Directional autonomy is measured in the direction of each module. Mean autonomy is an average using 1,000 random vectors in all directions. As the peak movement rate increases, directional autonomy rises, indicating more variation in the direction of selection. All plot points show mean values, and error bars span 2.5% and 97.5% quantiles for 10 populations under each peak movement rate, after 10,000 generations (population size $N_e = 5,000$, per locus mutation rate $\mu = 5 \times 10^{-4}$, pleiotropic effects mutation rate $\mu_B = 10^{-4}$, number of traits $p = 10$, number of loci $m = 500$, per locus mutation variance $\sigma = 0.02$, environmental variance $V_e = 0.8$, selection surface variance $V_\omega = 10$, selection surface within-module correlation $r_\omega = 0.8$, rate of peak movement per generation $\Delta_\theta = 0.0001 - 0.004$).

of the population's phenotypic covariance matrices showed an increase in variation associated with the second eigenvector, a contrast between modules (Fig. 2 and *SI Appendix*, Fig. S4 and Table S1).

Divergent directional selection efficiently created a modular variational structure in the populations. Even weak selection, peak movement on the order of 0.0005 SDs per trait per generation, was capable of creating detectable variational modularity after 10,000 generations. For larger peak movements, the effect was even quicker.

We can also use directional autonomy (*sensu* ref. 20) as a measure of variation in the direction of selection. Directional selection causes an increase in phenotypic (and genetic) variance associated with each module (Fig. 2).

Corridor Directional Selection. Although divergent directional selection is efficient at creating modular covariation patterns, selection acting simultaneously on all traits in a morphological structure in diverging directions is not a plausible scenario. A more realistic model is referred to as the "corridor model" of selection (21), where some traits undergo correlated directional selection but others are subject to stabilizing selection. In other words, corridor selection causes one set of traits to increase (or decrease) in size while keeping the rest constant.

In simulations of this scenario, the module under directional selection becomes much more integrated, while the module under stabilizing selection displays a slight increase in its correlations (Fig. 3). The between-module correlations fall, but not at the same rate as in the case of divergent directional selection. Corridor directional selection creates three correlation classes: high within-module correlations in the module under directional selection, intermediate within-module correlations in the module under stabilizing selection, and low correlations between modules, and it shows that simple selection regimes can create complex variational patterns.

Maintaining Modular Patterns. We also investigated what happens to modular patterns established by directional selection under three scenarios: drift, uncorrelated stabilizing selection, and correlated stabilizing selection. We took a single population subjected to strong divergent directional selection and used it as the starting point for 100 populations under each of these regimes. By measuring AVG Ratios over 10,000 generations (Fig. 4), we see that
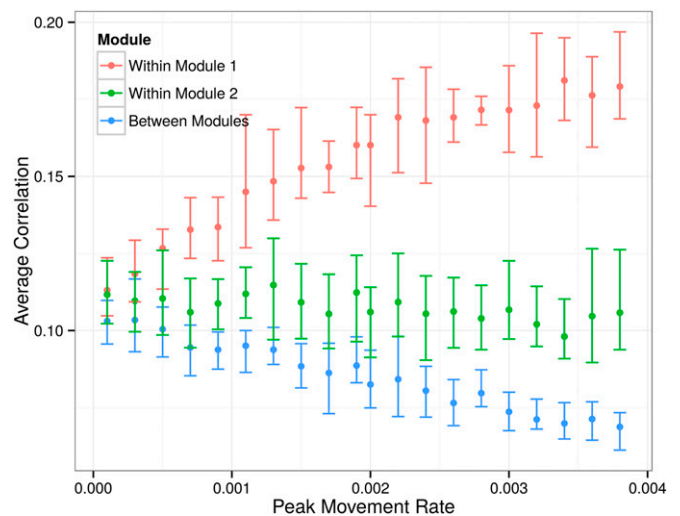

Fig. 3. Average correlation within and between modules under corridor selection. Faster peak movement promotes a higher differential between correlations in each group. Traits under directional selection become more correlated, whereas traits under stabilizing selection maintain the initial mean correlation. Between-module correlations fall proportional to peak movement rate. Points are mean values, and error bars span 2.5% and 97.5% quantiles for 10 populations under each peak movement rate after 10,000 generations. Parameter values are as in Fig. 2.
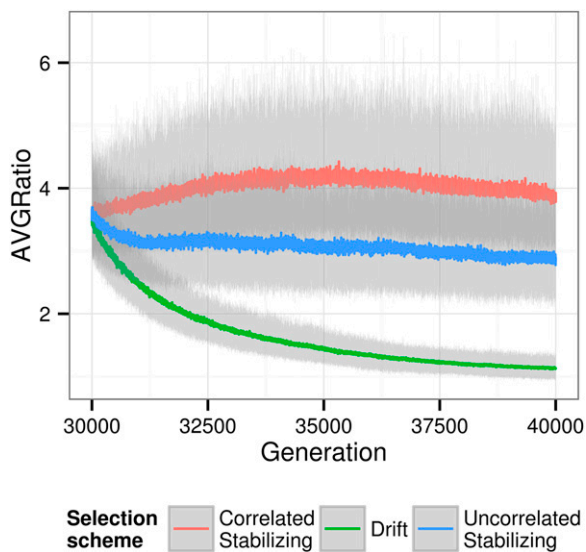
Fig. 4. AVG Ratio under drift and uncorrelated and correlated selection. The initial population had undergone divergent directional selection, so all populations start from a highly modular pattern. Mean values and 95% confidence intervals for 100 populations under each regime are given. Populations under drift quickly lose any modularity, whereas populations under stabilizing selection are able to maintain it for many generations. On average, correlated stabilizing selection maintains modularity at the same level established by directional selection, whereas under uncorrelated stabilizing selection, modularity decays to a lower level. Parameter values are as in Fig. 2, and $\Delta_\theta = 0.004$ for the initial population.

drift replicates quickly lose any trace of the strong modular pattern present in the initial population, whereas correlated stabilizing selection maintains and even increases the difference in between- and within-module correlations. Uncorrelated stabilizing selection allows a partial loss of modularity but could still maintain a modular pattern for many generations.

Discussion

We describe a model capable of simulating the evolution of a large number of quantitative traits based on an explicit genetic architecture. To our knowledge, our model is the first non-deterministic, individual-based model capable of incorporating many traits, large populations, mutation, drift, selection, and a variable heritable pleiotropic pattern. This complexity allows us to investigate the effect of different evolutionary processes, ranging from random genetic drift to several types of selection, such as stabilizing (correlated and independent) and directional selection (divergent and corridor).

Modularity has been associated with robustness (in the sense of resistance to perturbations) (22, 23) and evolutionary potential in biological systems, providing a genetic architecture that enables change to occur in parts of the organism without affecting other parts. The relationship between modularity, function, and development, as raised by the classic morphological integration hypothesis (5), suggests that selection should have considerable influence in creating the modular patterns we observe in nature (4). Even so, this hypothesis is controversial and difficult to test directly (24). We show that directional selection is a prime candidate for the engine behind the evolution of variational modularity, whereas stabilizing selection is critical for its maintenance.

Our results suggest that drift is incapable of producing or maintaining variational modular structures for many generations, even at the relatively large population sizes used (5,000 individuals). Furthermore, when drift produces modularity in one particular lineage at any given time, this pattern would not

be shared with other lineages and would be rapidly lost within that lineage. Stabilizing selection induces weak modularity in populations and provides more stability in these patterns compared with genetic drift.

The inability of stabilizing selection to create marked modular patterns in high dimensionality might seem unexpected, given that it has been shown to be effective in doing so for two-trait systems (17, 18). These results are in no way incompatible, and this agreement becomes more intuitive when we realize that the between-module correlations are not under selection and that this opposition of selected within-module correlations and neutral between-module correlations is only possible with more than two traits. Under correlated stabilizing selection, there is no advantage to low between-module correlations. This lack of advantage reduces the efficacy of stabilizing selection in creating variational modularity because it must rely solely on increasing within-module correlations. Directional selection, on the other hand, has a marked effect on the correlation between modules. Traits under directional selection in the same direction tend to become correlated, and traits under divergent selection tend to become uncorrelated. In other words, directional selection acts directly on the means of the traits and indirectly on the pleiotropic structures governing these traits (represented here by the **B** matrix; *Materials and Methods*), changing their pleiotropic behavior. Associations and constraints in the pleiotropic matrix are created and removed by directional selection, and this change in pleiotropic relations allows populations to respond efficiently to directional selection. We also show how directional selection on just a few traits (corridor selection) can create complex patterns of modularity.

Moreover, we show that stabilizing selection is essential for maintaining an established pattern of modularity, with correlated stabilizing selection performing this role efficiently. Correlated stabilizing selection can have many different causes, such as the necessity for cohesion among parts within an organism that impose selection on the associations between traits (3, 25, 26) or environmental and functional restrictions that also lead to stabilizing selection on the relations between traits. For example, the upper jaw and lower jaw must be the same size to allow proper mastication (26, 27). Directional selection acts on the variation maintained by these internal and external processes. The response to selection is affected by the pattern of covariation, because indirect selection, caused by genetic correlation between traits, deviates the phenotypic response to selection from the direction of the selection gradient (14, 26). At the same time, directional selection can, as we have shown here, also change the variational patterns dramatically, molding genetic covariation. Jones et al. (18) recently showed that epistatic relations can allow selection to favor mutations that align with the selection surface matrix for two traits. The authors argue that this finding implies mutations need not be neutral with respect to fitness but can be biased by previous selective history. Additionally, correlated directional selection has been implicated as a stabilizing force for G-matrices, but only when the direction of selection is aligned with variation in the population (15). In deterministic models, Pavlicev et al. (13) showed that correlated directional selection can cause indirect selection for an increase in correlation in two traits. We extend these results, showing that in the presence of variable pleiotropy, directional selection can realign a population's variance structure in the direction that facilitates a response to selection. Our results are unique in that we are able to explore these effects and gain valuable insight into systems with many dimensions while also allowing for novel interpretations of existing measurements of covariation.

The rapid evolution displayed by the covariation matrices in our simulations raises interesting questions compared with empirical measurements of phenotypic covariance matrices. There are reports of rapid divergence of G-matrices in some instances, for example, life history traits in nematodes (28) and pigmentation and physical dimensions in isopods (29). As for continuous

morphological traits, previous extensive comparative studies in the mammalian skull (30) indicate remarkable stability in the patterns of phenotypic and genetic (when available) covariation in the mammalian skull, despite extensive divergence in average phenotypes. These results suggest that shared function and development impose an internal stabilizing selection (5, 26) that plays a key role in keeping covariance structure stable across the mammalian radiation. Our results confirm this finding and reinforce the importance of stabilizing selection for the maintenance of covariance patterns. At the same time, the level of integration, measured by the average squared phenotypic correlation between all traits (r^2), is highly variable (30). For the same set of cranial traits, marsupials have r^2 values on the order of 0.3–0.5, whereas some primates (humans, gorillas, and chimpanzees) display values under 0.1 (30). These extreme differences have potentially important consequences for the evolution of these clades (31). Our results give indications as to how these differences could have arisen. Directional selection for size increase or decrease could cause the total average correlations to rise with no significant effect on the initial pattern of covariation. The same effect is observed in our simulations in the increase of within-module correlations between traits under correlated directional selection. Meanwhile, groups with low average correlations could have suffered events of directional selection not aligned with their previous modular structure. These predictions can be tested by reconstruction of net selection gradients and comparison of these gradients with current covariation structures. We predict that if the net selection gradient is aligned with the first eigenvector of the covariation matrix (i.e., selection on size), then integration should be higher.

There are several possible extensions to our model. As it stands, all loci recombine freely and the only parameter related to recombination is the number of loci. This simplification could be removed to explore the effects of linkage disequilibrium on the covariation between traits. It would then be possible for selection to create groups of loci and pleiotropic relationships with morphological traits that are inherited together. Other possible extensions are complexities in the genotype/phenotype relations, including nonlinearity or multiple levels of interaction between loci, explicitly including epistatic and dominance effects in the model, and could be helpful for understanding the evolution of genomic interactions.

Materials and Methods

Simulation Model. Our individual-based simulation approach is based on the model described by Wagner (32). A similar but simpler model by Reeve (33) can also be found. In Wagner's description (32), p phenotypic traits are controlled by m pleiotropic diploid loci. The m loci of an individual are represented by $2m$ real numbers (y_i with $i = 1 \ldots 2m$) representing some relevant physiological effect of locus i.

The translation from the physiological effects of y_i to additive effects (x_j with $j = 1 \ldots p$) is accomplished via an ontogenetic function: $\mathbf{x} = f(\mathbf{y})$, $f : \mathbb{R}^{2m} \to \mathbb{R}^p$. This function can be arbitrarily complicated and nonlinear. Assuming the function f is differentiable, we can take a linear approximation given by the differentiation of f, which is the matrix $\mathbf{B}$. The ontogenetic function then becomes: $\mathbf{x} = f(\mathbf{y}) = D[f(0)]\mathbf{y} = \mathbf{By}$. This approximation is equivalent to assuming that alleles only have additive effects (32). To make the simulation computationally tractable, we opted to simplify the ontogenetic $\mathbf{B}$ matrix even further. In our simulations, the $\mathbf{B}$ matrix is binary, coding only the influence (or lack of influence) of a particular locus on a particular trait. More clearly, if $\mathbf{B}_{ij}$ is 1, locus y_i influences additive effect x_j, and if it is 0, then it does not. Because the $\mathbf{B}$ matrix determines whether a genetic effect will influence one or more traits, it has also been called a pleiotropic matrix (34), but we point out that changes in pleiotropic relations can be mediated by epistatic interactions (12). So, although our model does not include epistasis explicitly, pleiotropic variation represented by the $\mathbf{B}$ matrix does so implicitly. It has been shown that negative pleiotropic effects (i.e., a single locus increasing a trait while decreasing another, and thus creating opposing relations between traits) can affect modularity patterns. In this scenario, the exact cancellation of positive (increasing or

decreasing traits simultaneously) and negative effects can lead to the absence of correlation between two traits (34). However, almost all pleiotropic QTLs detected for quantitative traits show only positive pleiotropic effects (35–37). Although some studies have reported negative pleiotropic loci (38), the resolution of these studies suggests that this finding might be due to closely linked loci (38). For this reason, we opted to include only two possible states for each position of the $\mathbf{B}$ matrix in our model, and if a locus affects more than one trait, it affects them in the same direction by the same amount.

To obtain the phenotypic value ($\mathbf{z}$), additive effects are added to an environmental deviation ($\mathbf{e}$), taken from a multivariate uncorrelated normal distribution with uniform variance V_e set to 0.8 in all dimensions. An individual's phenotype $\mathbf{z}$ is then given by: $\mathbf{z} = \mathbf{x} + \mathbf{e} = \mathbf{By} + \mathbf{e}$.

The ratio of the number of relevant loci (m) and the number of traits (p) determines the amount of recombination present in the model, because all loci recombine freely, without any chromosomal structure. The larger the value of m, the more independent recombination units we have in the simulated population.

Mutation rate is modeled by two different processes. With probability μ per locus per generation, the physiological effects y_i are altered by a random amount drawn from a normal distribution with a mean of 0 and variance σ set to 0.02. This mutation scheme implies a continuous allele model (39). In addition to this change in magnitude of the effect of the allele at each locus, we can flip the value of entries of the $\mathbf{B}$ matrix of each individual, with probability μ_B per generation per entry. Each position of the $\mathbf{B}$ matrix is independent.

Selection is modeled by a Gaussian individual selection surface $W(\mathbf{z})$, with predetermined multivariate optimum and covariance structure: $W(\mathbf{z}) = \exp\left[-\frac{1}{2}((\mathbf{z} - \theta)^T \omega^{-1}(\mathbf{z} - \theta))\right]$, where θ represents the multivariate fitness optimum and ω the covariance matrix of the selection surface. We simulate directional selection by altering the position of the optimum in phenotypic space. The rate of change in parameter θ represents different strengths of directional selection. If the covariance matrix ω is diagonal, then there is no correlated stabilizing selection, that is, selection directly on the covariance structure of the population. If ω is not diagonal, then there is correlated stabilizing selection and the association between traits is directly selected upon. Positive off-diagonal elements in the ω matrix promote positive correlations between traits in the population. The ω used in all simulations involving correlated stabilizing selection has a within-modules correlation r_ω set to 0.8 and null correlations between modules. The selective covariance V_ω is set to 10 for all traits. In cases with uncorrelated stabilizing selection, the off-diagonal elements were set to 0. This value of V_ω is consistent with strong stabilizing selection (16) (*SI Appendix*, Fig. S8).

A list of sires and dams is produced by sampling all individuals with replacement and probability proportional to their fitness $W(\mathbf{z})$. Sires and dams are then paired randomly and produce one offspring per couple. The offspring is created with gametes formed by sampling one allele of each of the m loci and the corresponding column of the individual's $\mathbf{B}$ matrix. This inheritance scheme means individual columns of the $\mathbf{B}$ matrix are inherited along with the corresponding sampled allele, so each allele carries its pleiotropic effects to the next generation. In a sense, this inheritance can be interpreted as *cis*-regulatory relations for pleiotropy. Population size N_e is kept constant at 5,000 individuals, and this selection scheme results in effective population size equal to census population size (40).

Initial parameter values were based on the parameter values used by Jones et al. (15–17). Values used maintained reasonable values for heritabilities (between 0.3 and 0.5) for morphological systems (41, 42). Additional simulations showing the stability of the results under different population sizes and mutation rates are presented in *SI Appendix*, Figs. S6 and S7.

Directional selection strength on univariate morphological systems was surveyed by Kingsolver et al. (43). Our strongest values of directional selection are on the weak side of a typical selection gradient for this survey, but we maintain the directional selection for many generations, leading to large morphological change in the populations. We vary the peak movement rate from 0.0001 to 0.004 for a period of 10,000 generations. Because the phenotypic variance fluctuated around 0.8–1.2, these peak movements can be interpreted in units of phenotypic SDs.

Quantifying Modularity. We detect variational modularity by investigating the phenotypic correlations between traits. A population is said to present variational modularity when the correlation between some sets of traits belonging to a module is higher than the correlation between traits of different modules. Average correlation between and within modules can be used to identify these differences. The ratio between the within- and between-module average

correlation is called the AVG Ratio, and it can be used to quantify the modularity in a population.

Changes in the population variational structure can be assessed by looking directly at the evolution of eigenvalues and associated eigenvectors of the phenotypic covariance matrix. These principal components measure how independent variation is distributed in phenotypic space. In most of our populations, the first eigenvector is in the direction associated with size, that is, the direction of simultaneous increase of all traits, whereas the second eigenvector is a contrast between modules or, more clearly, the direction of increase of traits within a module with simultaneous decrease in the other module (details are provided in *SI Appendix*).

We may also quantify the relative amount of variation in the direction of selection, excluding potentially constraining traits, and compare this directional measure with the mean amount of variation in all directions of morphological space. For this comparison, we use autonomy in the direction of the modules and compare it with the average autonomy for random directions (20). Directional autonomy of **G** in the direction of β is defined as $a(\mathbf{G},\beta) = (\beta\mathbf{G}^{-1}\beta)^{-1}(\beta\mathbf{G}\beta)^{-1}$.

1. Ancel LW, Fontana W (2000) Plasticity, evolvability, and modularity in RNA. *J Exp Zool* 288(3):242–283.
2. Han JDJ, et al. (2004) Evidence for dynamically organized modularity in the yeast protein-protein interaction network. *Nature* 430(6995):88–93.
3. Klingenberg CP (2008) Morphological integration and developmental modularity. *Annu Rev Ecol Evol Syst* 39:115–132.
4. Wagner GP, Pavlicev M, Cheverud JM (2007) The road to modularity. *Nat Rev Genet* 8(12):921–931.
5. Olson R, Miller E (1958) *Morphological Integration* (Univ of Chicago Press, Chicago).
6. Arnold SJ (1992) Constraints on phenotypic evolution. *Am Nat* 140(Suppl 1):S85–S107.
7. Walsh B, Blows MW (2009) Abundant genetic variation + strong selection = multivariate genetic constraints: A geometric view of adaptation. *Annu Rev Ecol Evol Syst* 40:41–59.
8. Arnold SJ, Bürger R, Hohenlohe PA, Ajie BC, Jones AG (2008) Understanding the evolution and stability of the G-matrix. *Evolution* 62(10):2451–2461.
9. Wagner GP (1996) Homologues, natural kinds and the evolution of modularity. *Amer Zool* 36(1):36–43.
10. Espinosa-Soto C, Wagner A (2010) Specialization can drive the evolution of modularity. *PLOS Comput Biol* 6(3):e1000719.
11. Clune J, Mouret JB, Lipson H (2013) The evolutionary origins of modularity. *Proc Biol Sci* 280(1755):20122863.
12. Pavlicev M, et al. (2008) Genetic variation in pleiotropy: Differential epistasis as a source of variation in the allometric relationship between long bone lengths and body weight. *Evolution* 62(1):199–213.
13. Pavlicev M, Cheverud JM, Wagner GP (2011) Evolution of adaptive phenotypic variation patterns by direct selection for evolvability. *Proc Biol Sci* 278(1713):1903–1912.
14. Lande R (1979) Quantitative genetic analysis of multivariate evolution, applied to brain: Body size allometry. *Evolution* 33(1):402–416.
15. Jones AG, Arnold SJ, Bürger R (2004) Evolution and stability of the G-matrix on a landscape with a moving optimum. *Evolution* 58(8):1639–1654.
16. Jones AG, Arnold SJ, Bürger R (2003) Stability of the G-matrix in a population experiencing pleiotropic mutation, stabilizing selection, and genetic drift. *Evolution* 57(8):1747–1760.
17. Jones AG, Arnold SJ, Bürger R (2007) The mutation matrix and the evolution of evolvability. *Evolution* 61(4):727–745.
18. Jones AG, Bürger R, Arnold SJ (2014) Epistasis and natural selection shape the mutational architecture of complex traits. *Nat Commun* 5:3709.
19. Revell LJ (2007) Testing the genetic constraint hypothesis in a phylogenetic context: A simulation study. *Evolution* 61(11):2720–2727.
20. Hansen TF, Houle D (2008) Measuring and comparing evolvability and constraint in multivariate characters. *J Evol Biol* 21(5):1201–1219.
21. Wagner GP (1984) Coevolution of functionally constrained characters: Prerequisites for adaptive versatility. *Biosystems* 17(1):51–55.
22. Hintze A, Adami C (2008) Evolution of complex modular biological networks. *PLOS Comput Biol* 4(2):e23.
23. Tran TD, Kwon YK (2013) The relationship between modularity and robustness in signalling networks. *J R Soc Interface* 10(88):20130771.
24. Lynch M (2007) The frailty of adaptive hypotheses for the origins of organismal complexity. *Proc Natl Acad Sci USA* 104(Suppl 1):8597–8604.
25. Hallgrímsson B, et al. (2009) Deciphering the Palimpsest: Studying the Relationship Between Morphological Integration and Phenotypic Covariation. *Evol Biol* 36(4):355–376.
26. Cheverud JM (1984) Quantitative genetics and developmental constraints on evolution by selection. *J Theor Biol* 110(2):155–171.
27. Figueirido B, Tseng ZJ, Martín-Serra A (2013) Skull shape evolution in durophagous carnivorans. *Evolution* 67(7):1975–1993.
28. Doroszuk A, Wojewodzic MW, Gort G, Kammenga JE (2008) Rapid divergence of genetic variance-covariance matrix within a natural population. *Am Nat* 171(3):291–304.
29. Eroukhmanoff F, Svensson EI (2011) Evolution and stability of the G-matrix during the colonization of a novel environment. *J Evol Biol* 24(6):1363–1373.
30. Porto A, Oliveira FB, Shirai LT, Conto V, Marroig G (2009) The evolution of modularity in the mammalian skull I. Morphological integration patterns and magnitudes. *Evol Biol* 36(1):118–135.
31. Marroig G, Shirai LT, Porto A, Oliveira FB, Conto V (2009) The evolution of modularity in the mammalian skull II. Evolutionary consequences. *Evol Biol* 36(1):136–148.
32. Wagner GP (1989) Multivariate mutation-selection balance with constrained pleiotropic effects. *Genetics* 122(1):223–234.
33. Reeve JP (2000) Predicting long-term response to selection. *Genet Res* 75(1):83–94.
34. Pavlicev M, Hansen T (2011) Genotype-phenotype maps maximizing evolvability: Modularity revisited. *Evol Biol* 38(4):371–389.
35. Leamy LJ, Routman EJ, Cheverud JM (1999) Quantitative trait loci for early- and late-developing skull characters in mice: A test of the genetic independence model of morphological integration. *Am Nat* 153(2):201–214.
36. Ehrich TH, et al. (2003) Pleiotropic effects on mandibular morphology I. Developmental morphological integration and differential dominance. *J Exp Zoolog B Mol Dev Evol* 296(1):58–79.
37. Cheverud JM (2004) *Modularity in Development and Evolution*, eds Schlosser G, Wagner G (Univ of Chicago Press, Chicago), pp 132–153.
38. Kenney-Hunt JP, et al. (2008) Pleiotropic patterns of quantitative trait loci for 70 murine skeletal traits. *Genetics* 178(4):2275–2288.
39. Crow JF, Kimura M (1964) The theory of genetic loads. *Proceedings of the XI International Congress of Genetics*, ed Geerts SJ (Pergamon, Oxford), pp 495–505.
40. Revell LJ (2007) The G matrix under fluctuating correlational mutation and selection. *Evolution* 61(8):1857–1872.
41. Mousseau TA, Roff DA (1987) Natural selection and the heritability of fitness components. *Heredity (Edinb)* 59(Pt 2):181–197.
42. Cheverud JM (1988) A comparison of genetic and phenotypic correlations. *Evolution* 42(5):958–968.
43. Kingsolver JG, et al. (2001) The strength of phenotypic selection in natural populations. *Am Nat* 157(3):245–261.

EVOLUTION

Melo and Marroig